Microscopic synchrotron X-ray analysis of mercury waste in simulated landfill experiments

AUTHOR(S):

Takaoka, Masaki; Kusakabe, Taketoshi; Shiota, Kenji; Hirata, Osamu; Kawase, Keizou; Yanase, Ryuji; Nitta, Kiyofumi

CITATION:

Takaoka, Masaki ...[et al]. Microscopic synchrotron X-ray analysis of mercury waste in simulated landfill experiments. Journal of Material Cycles and Waste Management 2023, 25(5): 2599-2611

ISSUE DATE:

2023-09

URL:

http://hdl.handle.net/2433/284916

Journal of Material Cycles and Waste Management (2023) 25:2599–2611
https://doi.org/10.1007/s10163-023-01632-9

SPECIAL FEATURE: ORIGINAL ARTICLE

Mercury cycles and their management

Microscopic synchrotron X-ray analysis of mercury waste in simulated landfill experiments

Masaki Takaoka[1] · Taketoshi Kusakabe[1] · Kenji Shiota[1] · Osamu Hirata[2] · Keizou Kawase[2] · Ryuji Yanase[2] · Kiyofumi Nitta[3]

Received: 19 December 2022 / Accepted: 19 February 2023 / Published online: 17 March 2023

Abstract

Mercury enters into the environment or waste streams because it is present as an impurity in natural minerals. Mercury must be appropriately managed as an hazardous waste. In this study, a waste layer of artificial mercury sulfide mixed with incinerator ash and sewage sludge compost in a simulated landfill experiment for 5 years was analyzed using microscopic synchrotron X-ray to obtain basic knowledge of mercury behavior in a landfill. Mapping by synchrotron X-ray revealed the distribution of mercury-containing particles in the waste layer. In most cases, the movement of mercury sulfide was not considered significant even within a microscopic range; however, water flows could enhance the movement of mercury sulfide particles. When disposing of mercury sulfide, "concentrated placement" or solidification, rather than mixing with other wastes, was more effective at preventing mercury leaching in lysimeters. The chemical form of mercury sulfide in each lysimeter was confirmed by X-ray absorption fine structure (XAFS) analysis, which showed that most of the mercury was present as metacinnabar and had not undergone any changes, indicating that it was extremely stable. The microscopic synchrotron X-ray analysis proved very useful for studying the behavior of mercury waste in a simulated landfill experiment.

Keywords Mercury sulfide · Landfill · Mapping · X-ray absorption fine structure

Introduction

The Minamata Convention on Mercury (MCM) entered into force in August 2017 with the aim of minimizing the effects on human health of environmental pollution by mercury. The convention had been ratified by 139 countries worldwide as of December 1, 2022 [1]. Trade in mercury, use of mercury in products and manufacturing processes, emissions to air, and release to water have been reduced under the MCM. Mercury is an impurity in natural resources emitted or released when coal is combusted, or when iron and zinc ores are processed. When the emissions and releases are reduced to the maximum extent possible, mercury migrates from air and water into waste. Mercury is an element and cannot be decomposed; therefore, it is important to manage it as a final waste product. In Japan, mercury is present as impurities in nonferrous metal ores, such as zinc ore, was recovered from sludge, refined, and exported overseas [2]. However, after the implementation of the MCM, its use in products decreased and it will eventually be phased out. It is now a requirement that mercury must be managed as an hazardous waste. In Japan, about 50 tons of mercury are generated as recovered mercury annually [3]. Mercury is generated at the 1000 ton/year level worldwide [3]. Safe long-term management of recovered mercury is a challenge. Storing it as metallic mercury has been implemented in the USA [4] and in the EU, recovered mercury is converted to mercury sulfide before being disposed of in waste salt mines [5]. However, suitable storage sites are not available in every country, and the best methods of disposal and management have not been fully elucidated; hence, more research is needed.

✉ Masaki Takaoka
takaoka.masaki.4w@kyoto-u.ac.jp

[1] Department of Environmental Engineering, Graduate School of Engineering, Kyoto University, C1-3, Kyotodaigaku-Katsura, Nishikyo-Ku, Kyoto 615-8540, Japan

[2] Environment Protection Center, Fukuoka University, 8-19-1, Nanakuma, Jyonan-Ku, Fukuoka 814-0180, Japan

[3] Japan Synchrotron Radiation Research Institute, SPring-8, 1-1-1 Kouto, Sayo, Hyogo 679-5198, Japan

Because it is difficult to dispose of metallic mercury, various mercury stabilization methods have been developed to convert metallic mercury into sulfide for disposal [6–10]. Mercury sulfide (cinnabar, α-HgS and metacinnabar, β-HgS) is a stable form of mercury in the natural environment; however, it is unclear whether mercury sulfide remains stable in real landfill environments. Yanase conducted landfill experiments on dry cell batteries including mercury using landfill simulators [11]. Over a 20-year period, the outflow of mercury from a lysimeter was $\leq 2\%$, and the major form of prelease was atmospheric dispersion via vaporization. The mercury content of the leachate was $< 0.2\%$. Batteries sampled after 10 and 20 years had suffered surface corrosion and about 6% of the mercury from the batteries had migrated to the waste layer.

We used similar types of landfill simulators to evaluate the stability of mercury sulfide, including that solidified with low alkali cement materials in a landfill [12, 13]. The outflow of mercury into leachate, atmospheric diffusion, and mercury methylation were investigated over a 5-year period. After the 5-year experiment, the lysimeters were disassembled, and the mass transfer characteristics of mercury in the landfilled mercury waste and residual mercury were investigated to determine the mass balance of mercury in the landfill [13]. When mercury sulfide was mixed with waste and disposed of in a landfill, the mercury content in the leachate was determined and the total elution rate was $< 0.1\%$ as shown in Table S1. When mercury sulfide was placed in layers in the center of the lysimeter, the mercury leaching rate was very low. However, the stratified distribution of total mercury after dismantling revealed that the semi-aerobic lysimeter had a high mercury content in the center of the lysimeter, which suggested mercury was not migrated. The lower part (lower-middle and lower layers) of the anaerobic lysimeter had a higher mercury content, which suggested a small amount of mercury was transported.

These studies only considered the behavior of mercury in air, water, and waste from a macro perspective; they did not investigate how mercury sulfide is dissolved or transported as a particle in the waste layer, and it is not known whether chemical changes of mercury sulfide particles occur. Some studies have examined the behavior of mercury in actual landfills [14–20], but most measured it in leachate or landfill gas; few have analyzed mercury in landfilled waste [17, 18]. While some studies have investigated the leachability of mercury sulfide in landfills, little is known about the changes related to mercury sulfide [21, 22].

In this study, it was assumed that mercury migration was probably very limited based on the low leachability of mercury sulfide and results of our previous research [13]. Mapping of mercury by synchrotron X-ray was conducted using microbeams and the chemical form of mercury was determined using X-ray absorption fine structure (XAFS) analysis. A cross-section of the lysimeter was prepared to confirm whether the phenomena were consistent with those seen from a macroscopic perspective [13], and to obtain basic knowledge of mercury behavior in a landfill.

This also enabled us to determine if the degree of advection and diffusion of mercury persists at the microscale. It was assumed that the chemical state of the mercury would change as it spread from the original artificial mercury sulfide to its surroundings. An XAFS analysis using high-brilliance synchrotron radiation was used to determine the chemical state, because it is not necessarily the case that a highly crystalline material forms in the portion that leaches out of artificial mercury sulfide and is advected or diffused. Recently, XAFS analyses have been applied to determine the speciation of mercury in contaminated soil [23, 24] and mine wastes [25, 26]. Despite these studies, little information is available on the speciation of mercury in landfilled waste.

Materials and methods

Sample

Twelve landfill simulator lysimeters containing mercury waste were assembled. Two different mercury wastes were prepared: artificial mercury sulfide and mercury sulfide solidified with a low alkali cement material. The lysimeters were filled with these mercury wastes together with two types of typical landfilled waste: incineration ash only and a mixture of incineration ash (80%) and sewage sludge compost (20%). The mercury content was approximately 1% in the waste materials.

Two different techniques were adopted to landfill the mercury waste: mixing of the mercury sulfide with other waste, and a “bedded pattern” in which the mercury sulfide or solidified materials were embedded as the middle layer. All lysimeters were prepared as semi-aerobic or anaerobic landfills. We also conducted blank tests for each type of landfill. The experimental setup of the landfill simulating lysimeters was shown in two previous studies [12, 13]

Thirty samples were taken from the surface, middle, and lower layers of the mixed waste lysimeter for the synchrotron-based mapping analysis, while in the lysimeter with a bedded pattern, the analysis focused on the bedded layer and area below that layer. The sample numbers are listed in Table 1.

Samples were vacuum-sealed after sampling and submitted for analysis. Photographs of the samples are shown in Figure S1. Measurements of each sample were made while maintaining the vertical orientation of the lysimeters.

Table 1 Samples for synchrotron X-ray mapping and XAFS analysis

Landfill type & waste	Location	Mix	Map	XAFS	Bedded	Map	XAFS	Cement solidifcation	Map	XAFS	Blank	Map	XAFS
Semi-aerobic	Surface	1-SISM-0	○	○	2-SISBe-0	–	–	3-SISC-0	–	–	4-SISBl-0	–	–
		1-SISM-3	–	–	2-SISBe-3	○	–	3-SISC-3	–	–	4-SISBl-3	–	–
	Middle	1-SISM-4	○	○	2-SISBe-4	○	○	3-SISC-4	○	○	4-SISBl-4	○	–
Waste: IA + SSC		1-SISM-5	–	–	2-SISBe-5	○	–	3-SISC-5	○	–	4-SISBl-5	–	–
	Bottom	1-SISM-8	○	○	2-SISBe-8	○	–	3-SISC-8	○	–	4-SISBl-8	–	–
Anaerobic	Surface	5-AISM-0	○	○	6-AISBe-0	–	–	7-AISC-0	–	–	8-AISBl-0	–	–
		5-AISM-3	–	–	6-AISBe-3	○	–	7-AISC-3	–	–	8-AISBl-3	–	–
	Middle	5-AISM-4	○	○	6-AISBe-4	○	○	7-AISC-4	○	○	8-AISBl-4	○	–
Waste: IA + SSC		5-AISM-5	–	–	6-AISBe-5	○	–	7-AISC-5	○	–	8-AISBl-5	–	–
	Bottom	5-AISM-8	○	○	6-AISBe-8	○	–	7-AISC-8	○	–	8-AISBl-8	–	–
Semi-aerobic	Surface	9-SIM-0	○	○							10-SIBl-0	–	–
	Middle	9-SIM-4	○	○							10-SIBl-4	○	–
Waste: IA	Bottom	9-SIM-8	○	○							10-SIBl-8	–	–
Anaerobic	Surface	11-AIM-0	○	○							12-AIBl-0	–	–
	Middle	11-AIM-4	○	○							12-AIBl-4	○	–
Waste: IA	Bottom	11-AIM-8	○	○							12-AIBl-8	–	–

– Not analyzed

Measurement methods

(1) Synchrotron based mapping measurement

The X-ray measurements were performed using the BL37XU beamline at SPring-8, which is a synchrotron radiation facility in Japan [27]. The X-ray energy was set to 12.5 keV. The sealed sample shown in Figure S1 was attached to a sample holder and fixed at the irradiation position. After confirming the position with a camera, the sample was irradiated with X-rays, and fluorescent X-rays were detected by a multi-element silicon drift detector. The settings are shown in Figure S2.

The sample was mapped with a beam focused to 209×152.5 nm at 1-μm intervals, covering an area of 50×100 μm. Because BL37XU is capable of high-speed X-ray fluorescence mapping of several elements, the X-ray fluorescence of each element was acquired in each channel. For mercury, the Lα and Lβ spectral lines were recorded separately. After acquiring the data, hot spots were visualized using the LabVIEW software (National Instruments Corporation, USA) installed in BL37XU at SPring-8, to determine whether the hot spots were mercury-derived based on the distribution of Lα and Lβ of mercury. Detailed mapping was performed in an area of $10-20 \times 10-20$ μm at 0.2-μm intervals for areas of high X-ray fluorescence intensity originating from mercury. These mapping results confirmed the advection and diffusion of mercury from mercury sulfide for each layer.

(2) XAFS measurement

Initially, we attempted to perform XAFS measurements with the same beam size as used for the mapping, but we could not obtain a good spectrum and therefore abandoned XAFS measurements for each location obtained from each mapping, and performed XAFS measurements for each layer over a slightly wider area (927×960 μm). Because of the quality of the spectra, we focused our measurements only on the X-ray absorption near edge spectroscopy (XANES) region. For each layer, the spectra of Hg L-III were collected in fluorescence mode using a multi-element silicon drift detector for the landfilled samples, and in transmission mode using an ionization chamber for the reference materials (cinnabar, meta-cinnabar, $HgSO_4$, and Hg_2SO_4).

Data analysis method

(1) Analysis of mapping data

The Ch1 HgLα data were displayed in 32-bit color using ImageJ software (NIH, USA). After inversion, rotation, and other forms of processing, we confirmed that the images were consistent with those displayed in the LabVIEW software installed in BL37XU.

In some cases, the images did not show the presence of the mercury sulfide added to the landfilled waste because of shading in a particular measurement range. Therefore, for mapping data in the 50×100 μm range, the X-ray fluorescence intensity of mercury in blank samples from one of the landfill experiments (incineration ash [80% + sewage sludge compost [20%]: 4-SISBl-4 and 8- AISBl -4; incineration ash only: 10-SIBl-4 and 12-AIBl-4) was measured. If the intensity of the bright spot exceeded the highest X-ray fluorescence intensity of mercury for the blank samples, we determined that the spot was affected by mercury sulfide. We counted the spots meeting this criterion in each sample. In addition, an average value for the entire mapping surface was calculated to shed light on the presence and movement of mercury.

(2) Analysis of XAFS data

The XANES spectra between 11,957 and 12,381 eV were analyzed by Athena software [28]. The spectra of reference materials and landfilled samples were compared, and their spectral shapes were used to identify the major species (because a XANES spectrum reflects the local environment of elements within a material). Chemical species were also distinguished using linear combination fitting (LCF) technique with black mercury sulfide (meta-cinnabar) and red mercury sulfide (cinnabar) [29].

Results and discussion

Mercury distributions in the lysimeters

(1) Blank sample

The results for the blank sample from the mapping data in the 50×100 μm range are shown in Fig. 1. A larger area of shading for Hg Lα was observed in 10-SIBl-4 compared with the other samples. The highest X-ray fluorescence intensities of Hg Lα were 934, 505, 415, and 3,189 for 4-SISBl-4, 8-AISBl-4, 10-SIBl-4, and 12-AIBl-4, respectively.

The shading intensity was not only due to the mercury concentration; it was also influenced by other elements. Figure 2 shows the distribution of Hg Lα and Hg Lβ for 10-SIBl-4 and 12-AIBl-4. For 10-SIBl-4, there was a clear lack of discrepancy in the upper shading area between Hg Lα and Hg Lβ. For 12-AIBl-4, there was a bright spot for Hg

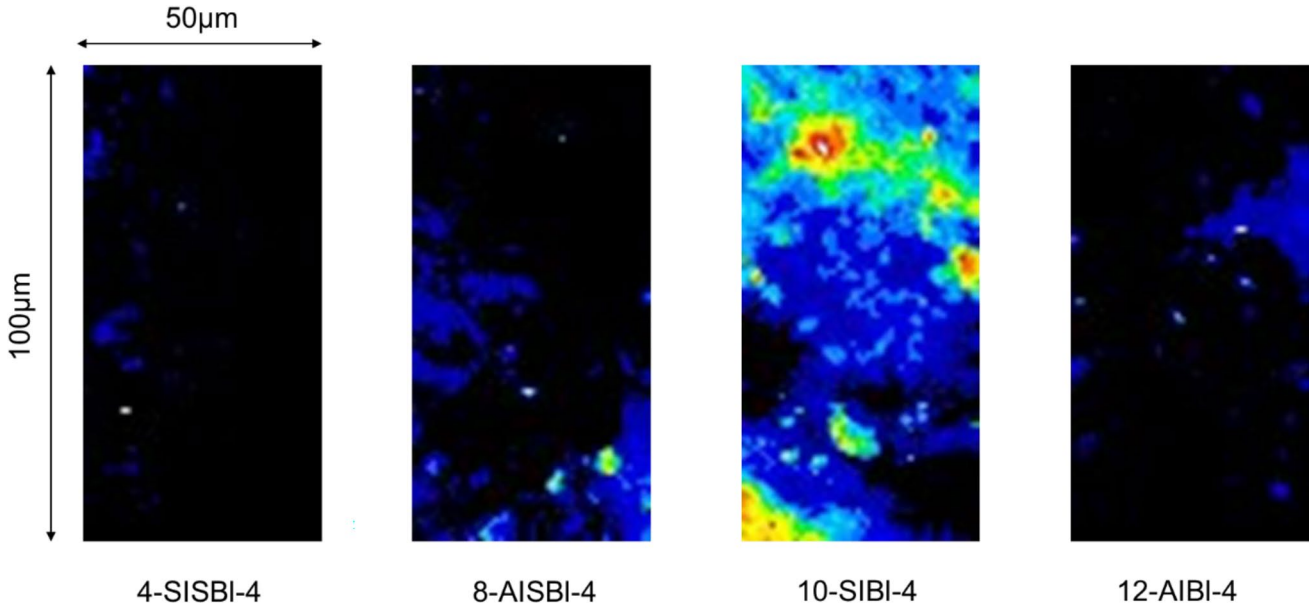

Fig. 1 Mapping analysis of HgLα in blank samples

Lα in the upper left center, consistent with Hg Lβ. A detailed analysis (10 × 10 μm) of this spot showed clear agreement with Hg Lβ, indicating the presence of mercury. These samples were not made with the addition of artificial mercury sulfide. Therefore, we can conclude that the particles contained mercury that was present in the original waste. The size of the particles in which mercury was concentrated was about 1 − 2 μm. The wastes used in this study were incineration ash and sewage sludge compost. Takaoka et al. reported that the predominant species of mercury in the fly ash from municipal solid waste incineration was Hg_2Cl_2, based on XANES analysis [30]. According to Vogel et al., XANES showed that the major inorganic mercury compounds in sewage sludge ash were HgS, $HgCl_2$, and HgSe [31]. The forms of mercury that did not run off even with artificial rainfall during the simulated landfill experiment were considered to be highly insoluble, such that $HgCl_2$ was unlikely to be present. Therefore, the data obtained by this mapping indicated that measurement points with an intensity of ≥ 3190 were affected by the artificially added mercury sulfide.

(2) Mixed waste samples

Figure 3 shows the distribution of mercury-containing particles in the semi-aerobic landfill layer (1-SISM) of mercury sulfide with incineration ash and sewage sludge compost. 1-SISM-0 was a sample from the top of the simulated landfill lysimeter, 1-SISM-4 was from the middle layer, and 1-SISM-8 was a sample from the bottom of the lysimeter. In the 50 × 100 μm area, some mercury-containing particles and groups of particles were observed. The mapping result for one of the particles is shown in Fig. 3. Particle size varied but most were 5 − 7 μm in length and 3 − 5 μm in width. The size variations were likely due to differences in the degree of agglomeration of the artificial mercury sulfide. Particle migration and advection/diffusion of mercury therefrom was also possible. The shading corresponding to the Hg Lα intensity was less diffuse, which suggested that the mercury had not dissolved and spread out. This was also the case for the middle and lower layers, where there were differences in the number of particles because of the limited area targeted and difficulty of analyzing a uniform surface. Differences in the behavior of the particles were not considered.

Figure 4 shows the distribution of mercury-containing particles in the anaerobic landfill layer (5-AISM) of mercury sulfide with incineration ash and sewage sludge compost. It is basically the same as Fig. 3, with some mercury-containing particles and groups of particles being observed. There was no spreading of mercury from these particles, which suggested that the anaerobic conditions might not have affected the migration of mercury sulfide.

Figures 5 and 6 show the distribution of mercury-containing particles in the semi-aerobic landfill layer (9-SIM) and anaerobic landfill layer (11-AIM) of incineration ash with mercury sulfide, respectively. Both figures show that many mercury-containing particles were present in the middle layer (9-SIM-4 and 11-AIM-4), which was probably coincidental, but in both cases they were aligned vertically. In landfills, there is a layer of high permeability, which is referred to as the water path [32, 33]. It is possible that landfills with incineration ash may contain areas where liquids can flow easily, such as a water path, but the analysis was

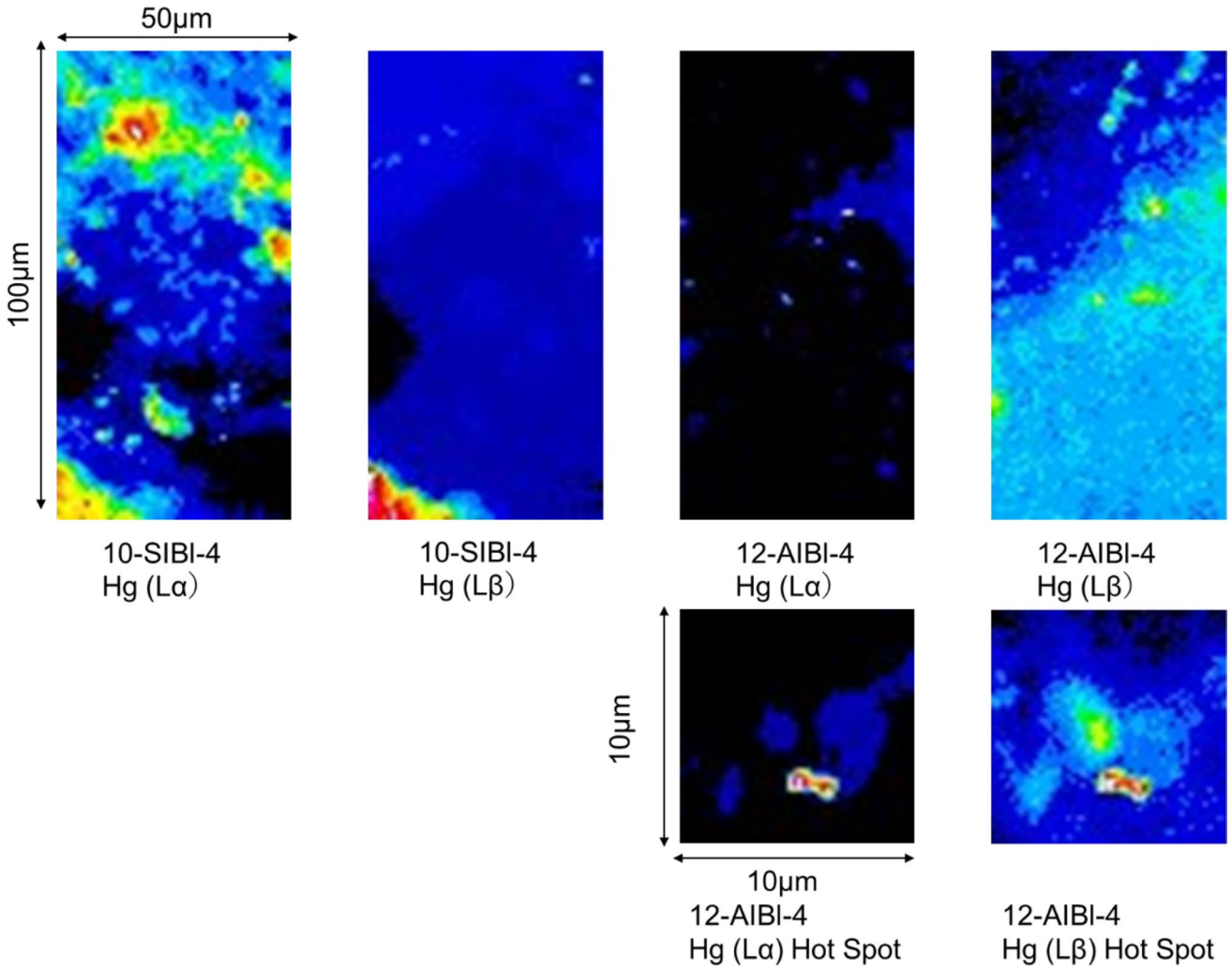

Fig. 2 Mapping analysis of Hg Lα and Hg Lβ in samples 10-SIBl-4 and 12-AIBl-4

inconclusive because only two areas were analyzed. However, the distribution of mercury could be interpreted as reflecting movement of particles along the water path, in the process of which the blue area may have been contaminated by a very small amount of dissolved constituents. It was difficult to detect differences between the semi-aerobic and anaerobic conditions.

(3) **Mercury sulfide or solidified mercury sulfide with low-alkaline cement placed in the middle of the lysimeter**

The mercury distribution in the experiments in which mercury sulfide(2-SISBe: semi-aerobic, 6-AISBe: anaerobic) or cement-solidified mercury sulfide (3-SISC: semi-aerobic, 7-AISC: anaerobic) was placed in the center of the lysimeter was very different from that in the experiments in which mercury sulfide was mixed with other wastes, such as incineration ash and sewage sludge compost. In the experiments with bedded mercury sulfide, very few (1–2) particles about 1 μm in size were observed. Figure 7 shows the mercury-containing particles in the layer below the mercury bedded area. Only 7-AISC had particles in the middle to lower layers, and they were not observed in the lowest layer.

It is possible that the particles in the layer below the mercury bedded area were either from the original landfill waste or from particles that had run off from the bedded mercury sulfide areas. This suggests that little mercury had dissolved and become mobile. Even when mercury sulfide was solidified by the low-alkaline cement, mercury in the leachate was detectable in the first period [12.13]. This suggests that some of the mercury sulfide powder had adhered to the surface of the cement during solidification in its production and might have later been removed by the artificial rainfall.

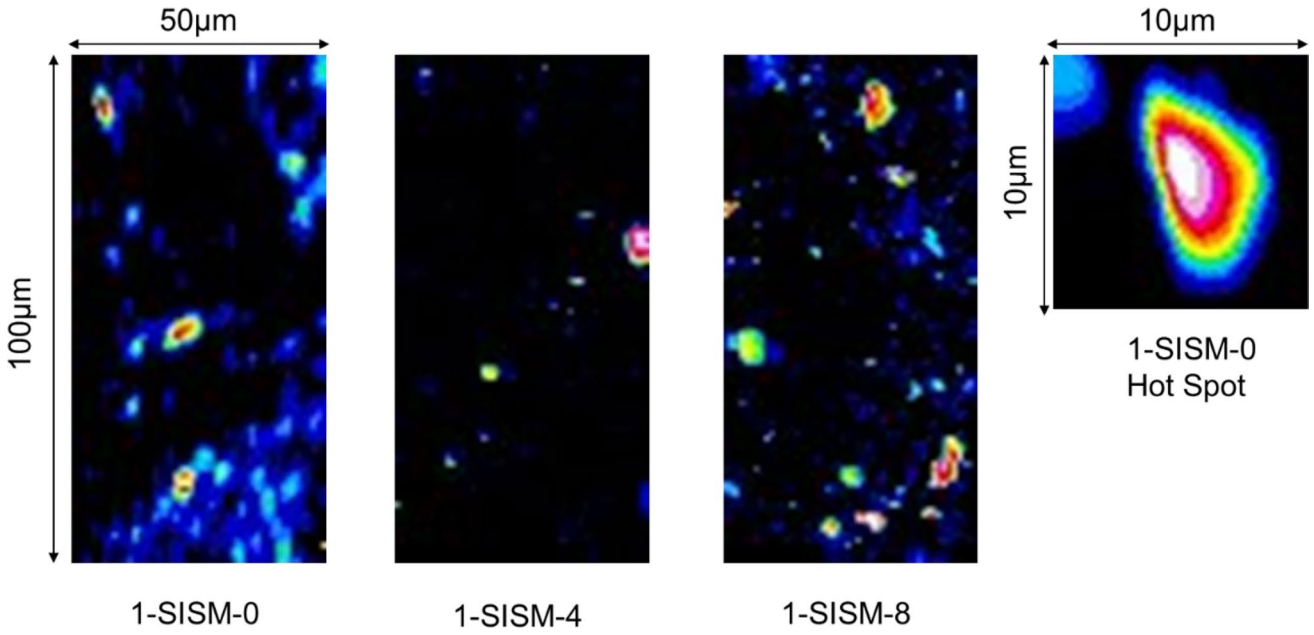

Fig. 3 Distribution of mercury-containing particles in the semi-aerobic landfill layer (1-SISM) of mercury treated with incineration ash and sewage sludge compost

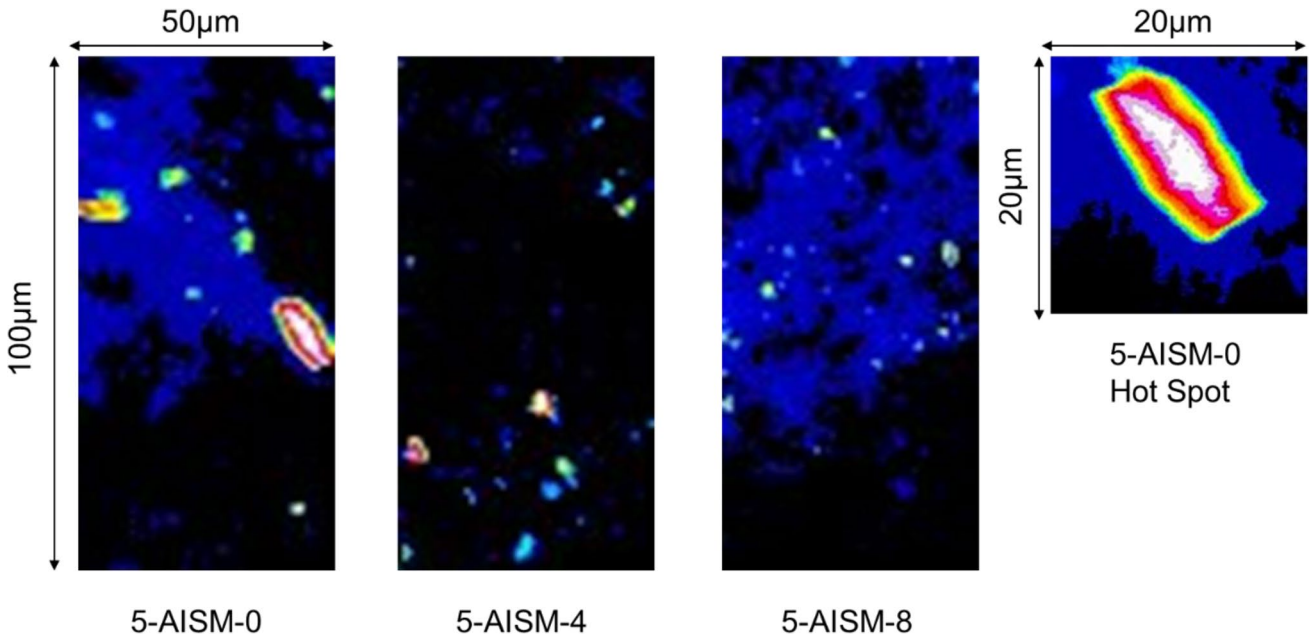

Fig. 4 Distribution of mercury-containing particles in an anaerobic landfill layer (5-AISM) of mercury treated with incineration ash and sewage sludge compost

Number of mercury sulfide particles present in each layer of the lysimeters

We attempted to quantify the mapping data to determine whether mercury sulfide particles were migrating from the top to the bottom of the lysimeter. The pixels with an intensity > 3190, i.e., the boundary value of the original waste-derived mercury value obtained from the background, were counted among the 5,000 pixels that were mapped (50 × 100 μm area). The percentage was calculated by dividing by the original number of pixels (5000).

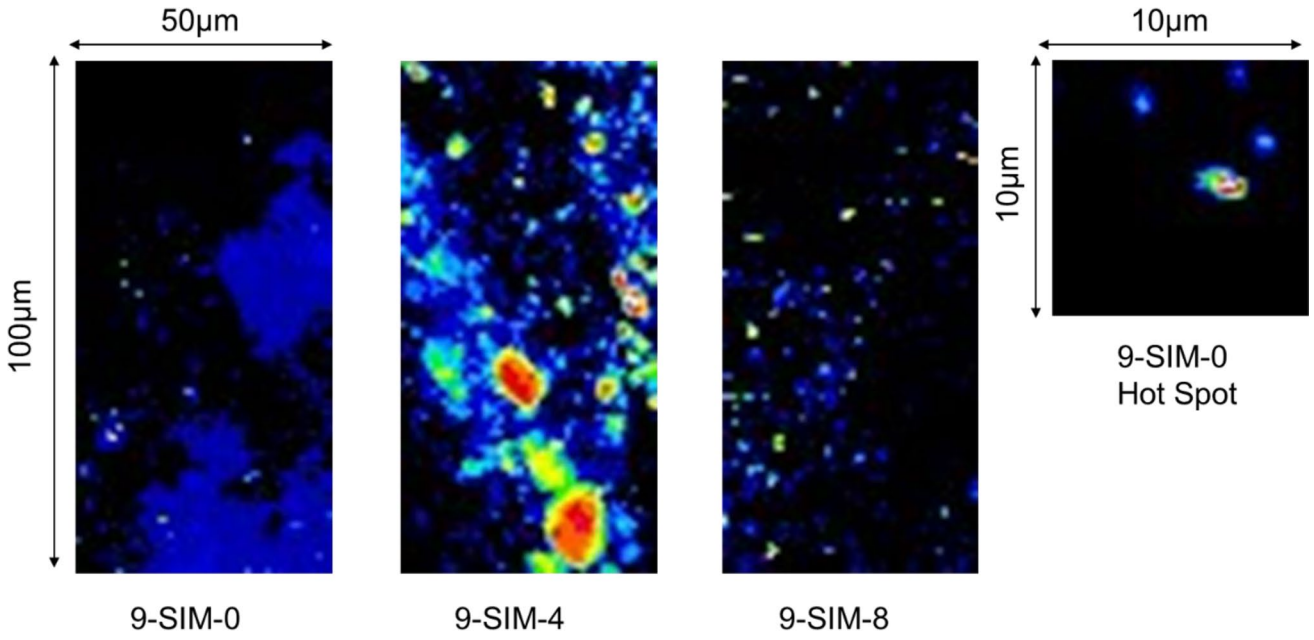

Fig. 5 Distribution of mercury-containing particles in the semi-aerobic landfill layer (9-SIM) mixed with incineration ash and mercury sulfide

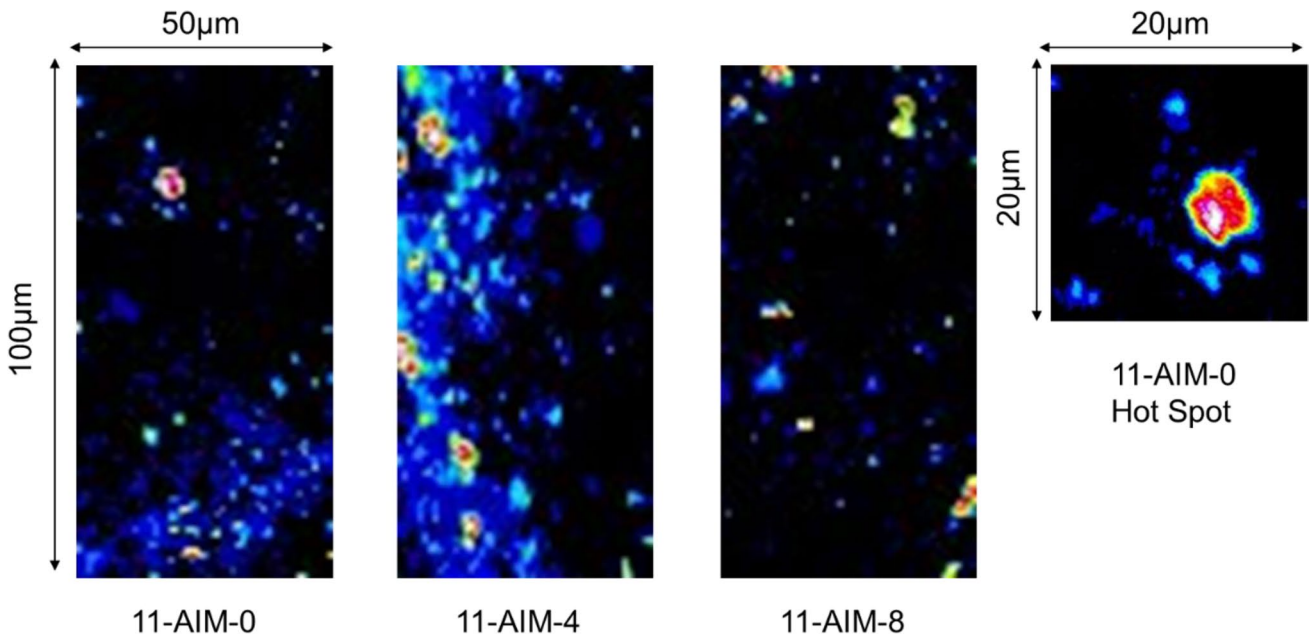

Fig. 6 Distribution of mercury-containing particles in the anaerobic landfill layer (11- AIM) mixed with incineration ash and mercury sulfide

The results are shown in Table 2. Averages are shown for layers in which multiple ranges were analyzed. In layer 5-AISM-0, four mappings were performed, with an average of 4.5% and standard deviation of 6.3%. The standard deviation was high because the particles were unevenly distributed at the micro-scale. Although a full quantitative assessment was not possible, we could nevertheless see a difference between the mixed mercury sulfide case and bedded mercury sulfide case including cement solidification. It was initially presumed were fewer mercury-containing particles in the upper layers, and that the number of mercury-containing particles may have increased toward the lower layers since the rain was artificially made to fall, but the data from layers 1-SISM, 5-AISM, 9-SIM,

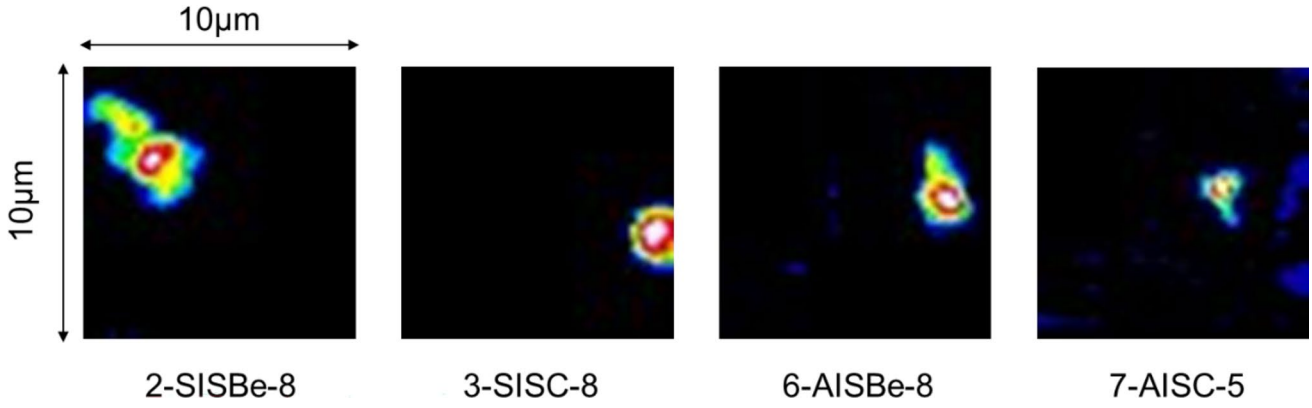

Fig. 7 Detection of mercury-containing particles in the layer below the mercury burial area in the experiments in which mercury sulfide (2-SISBe: semi-aerobic, 6-AISBe: anaerobic) or cement-solidified mercury sulfide (3-SISC: semi-aerobic, 7-AISC: anaerobic) was placed in the center of the lysimeter

Table 2 Percentage of mercury originating from the mercury sulfide added to each layer of the lysimeters

Landfill type & waste	Location	Mix	Percetage (%)	Bedded	Percetage (%)	Cement solidification	Percetage (%)	Blank	Percetage (%)
Semi-aerobic	Surface	1-SISM-0	7.1	2-SISBe-0	–	3-SISC-0	–	4-SISBl-0	–
		1-SISM-3	–	2-SISBe-3	0	3-SISC-3	–	4-SISBl-3	–
	Middle	1-SISM-4	2.1	2-SISBe-4	100	3-SISC-4	82.6	4-SISBl-4	0
Waste: IA + SSC		1-SISM-5	–	2-SISBe-5	0	3-SISC-5	0.02	4-SISBl-5	–
	Bottom	1-SISM-8	13.8	2-SISBe-8	0	3-SISC-8	0	4-SISBl-8	–
Anaerobic	Surface	5-AISM-0	4.5	6-AISBe-0	–	7-AISC-0	–	8-AISBl-0	–
		5-AISM-3	–	6-AISBe-3	0	7-AISC-3	–	8-AISBl-3	–
	Middle	5-AISM-4	4.6	6-AISBe-4	0*	7-AISC-4	100	8-AISBl-4	0
Waste: IA + SSC		5-AISM-5	–	6-AISBe-5	0	7-AISC-5	0	8-AISBl-5	–
	Bottom	5-AISM-8	3.9	6-AISBe-8	0	7-AISC-8	0	8-AISBl-8	–
Semi-aerobic	Surface	9-SIM-0	0.1					10-SIBl-0	–
	Middle	9-SIM-4	50.2					10-SIBl-4	0
Waste: IA	Bottom	9-SIM-8	2.2					10-SIBl-8	–
Anaerobic	Surface	11-AIM-0	5.8					12-AIBl-0	–
	Middle	11-AIM-4	30.8					12-AIBl-4	0
Waste: IA	Bottom	11-AIM-8	5.5					12-AIBl-8	–

*The lower portion of the bedded mercury sulfide was analyzed

– Not analyzed

and 11-AIM with mixed mercury sulfide showed that there was no consistent trend, suggesting that the mercury-containing particles largely remained in their original location. This suggests that most of the mercury-containing particles remained in their original location.

The 2-SISBe and 6-AISBe lysimeters with bedded mercury sulfide did not have any high mercury concentration spots, even in the top layer. It was assumed that, under anaerobic conditions with a saturated moisture layer, upward migration of pollutants due to evaporation of water at the surface of the landfill site would occur [34], but there were no points with a high mercury concentration at the top of the lysimeters. It was, therefore, assumed that the amount dissolved was extremely small.

The volatilization of mercury has also been observed in actual landfills [14, 35]. In a previous study, we also found a constant stream of vaporized mercury [12, 13]; however, it was not vaporized to the extent that points with a high mercury concentration were visible. The 2-SISBe-4, 3-SISC-4, and 7-AISC-4 results indicated that there was a high mercury concentration because the layers containing mercury sulfide or solidified material were analyzed. The

6-AISBe-4 results showed zero intensity because the lower portion of the bedded mercury sulfide was analyzed rather than the mercury waste layer, but this does not mean that mercury was not present. The 3-SISC and 7-AISC results also showed no points with a mercury intensity greater than the naturally occurring background, with no mercury being detected in the layers below the cement solidification. The results for 3-SISC and 7-AISC indicated that mercury was not detected at any point during cement solidification. These results indicated that most of the mercury-containing particles in the landfill were immobile. When disposing of mercury sulfide, "concentrated placement" or solidification, rather than mixing with other wastes, is more effective for preventing mercury leaching.

Chemical form of mercury in the lysimeter

Although it was not possible to analyze each particle individually to determine the chemical form of mercury, an XANES analysis of mercury was performed at locations in the surface, middle, and lower layers of lysimeters with mixed waste and mercury sulfide (1-SISM, 5-AISM, 9-SIM, and 11-AIM). The Hg LIII absorption edge XANES spectra in each sample and reference materials are shown in Fig. 8. Figure 8 suggests that all of the absorption edges could be represented by metacinnabar, which is a very stable compound abundant in soil and sediments [35]. Because most of the mercury in the original mercury treatment was metacinnabar [8], it was concluded that no detectable changes in the mercury occurred during the 5-year period.

The Hg LIII absorption edge XANES spectra in the middle layer of all lysimeters are shown in Fig. 9. Mercury

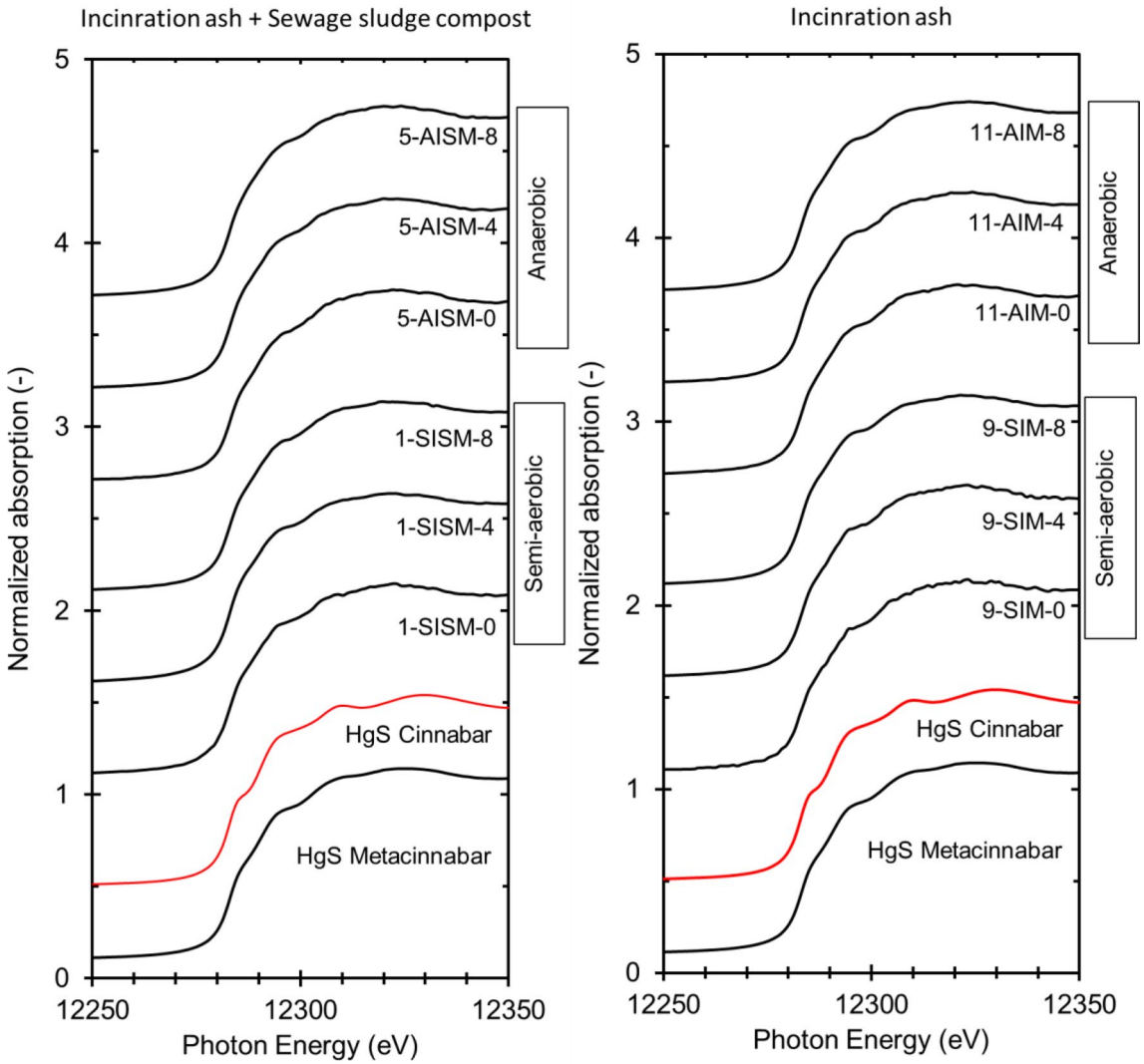

Fig. 8 The Hg LIII absorption edge XANES spectra of mercury in each layer of the lysimeters with mixed waste and mercury sulfide

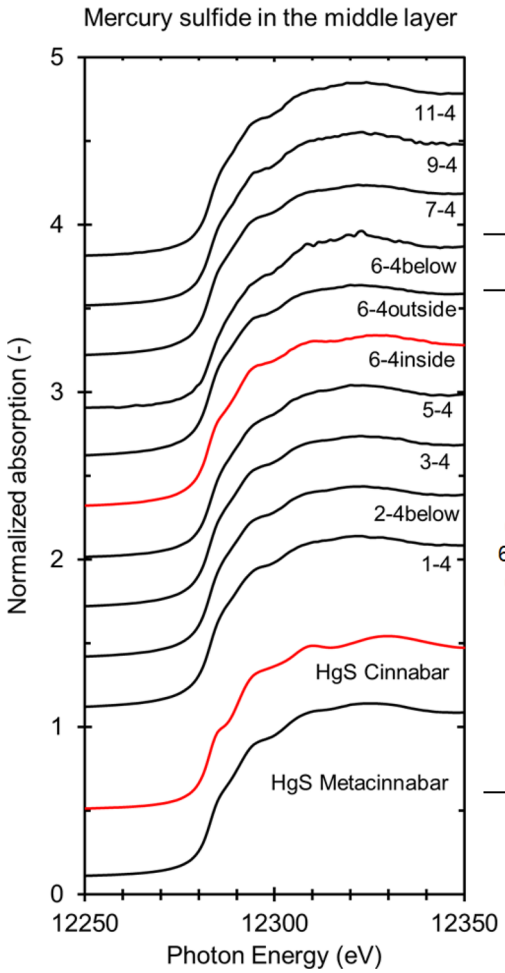

Sample	Cinnabar (−)	Meta−cinnabar (−)	Rfactor
1_SISM_0	0.00	1.00	0.0028
1_SISM_4	0.00	1.00	0.0072
1_SISM_8	0.00	1.00	0.0017
2_SISBe_4	0.00	1.00	0.0078
3_SISC_4	0.00	1.00	0.0067
5_AISM_0	0.00	1.00	0.0005
5_AISM_4	0.00	1.00	0.0016
5_AISM_8	0.00	1.00	0.0042
6_AISBe_4inside	0.32	0.68	0.0068
6_AISBe_4outside	0.00	1.00	0.0093
6_AISBe_4below	0.00	1.00	0.0026
7_AISC_4	0.00	1.00	0.0054
9_SIM_0	0.00	1.00	0.0011
9_SIM_4	0.00	1.00	0.0012
9_SIM_8	0.00	1.00	0.0038
11_AIM_0	0.00	1.00	0.0005
11_AIM_4	0.00	1.00	0.0016
11_AIM_8	0.00	1.00	0.0026

Fig. 9 The Hg LIII absorption edge XANES spectra of mercury in the middle layer in all lysimeters and the LCF results

species in all samples except 6-AISBe-4 were metacinnabar. Because the 6-AISBe-4 sample clearly showed a change in color tone on the inside and outside of the sample, the analysis was performed for each side. The LCF results showed that the inner part where this color change was observed contained 32% cinnabar, while the other parts contained 100% metacinnabar. 6-AISBe was a sample obtained from a lysimeter under anaerobic conditions, and it was possible that a crystalline structural change occurred in the part of the sample with a color change. Although Dickson et al. reported that the transformation of metacinnabar to cinnabar occurs at 344 °C [36], no increase in temperature was observed in this experiment. Although other factors might have played a role in the transformation of metacinnabar, they could not be determined in this study.

Although this study shows that artificial mercury sulfide is unlikely to change in a simulated landfill environment over a 5-year period, this can be further confirmed by examining various factors affecting mercury leaching, conducting accelerated leaching tests and other evaluations of the artificial mercury sulfide for safe final disposal. The efforts will lead to identify technical requirements for the stabilization process and long-term safe disposal of mercury waste.

Conclusions

In this study, an artificial waste layer of mercury sulfide mixed with incinerator ash and sewage sludge compost was placed in a simulated landfill experiment for 5 years and then analyzed microscopically using synchrotron X-ray. Mapping by synchrotron X-ray revealed the distribution of mercury-containing particles in the waste layer. Even if mercury sulfide was mixed with incinerator ash or sewage sludge compost, the amount of mercury leached from the mercury sulfide particles and contaminating the surroundings was minimal. Although the particles themselves could be leached out by artificial rainfall, their movement was not considered significant. However, in the lysimeters where

incinerator ash and mercury sulfide were mixed, water paths might be formed and movement of mercury sulfide particles occurred. When mercury sulfide or mercury sulfide solidified with low-alkaline cement was placed in the center of the lysimeters, almost no mercury sulfide particles were detected in the lower part of the lysimeter, confirming that there was almost no mercury leaching or migration of the mercury sulfide particles. Additionally, no areas of mercury enrichment were detected in the top layers due to upward migration. These results were consistent with those of previous studies, including the changes in mercury concentration in leachate over time.

The chemical form of mercury in each lysimeter was confirmed by XANES analysis, which showed that most of the mercury was present as metacinnabar and had not undergone any changes; this indicated that it was extremely stable. Some of the mercury sulfide changed to cinnabar inside the bedded mercury sulfide only in a simulated landfill experiment where mercury sulfide was placed in the center of the lysimeter and kept under anaerobic conditions. The reasons for this change were not investigated and further investigation is required.

This study confirmed that, when disposing of mercury sulfide, "concentrated placement" or solidification, rather than mixing with other wastes, is more effective for preventing mercury leaching. In the future, it will be necessary to conduct similar experiments on other solidified materials and develop a landfill method with less mercury leakage. In addition, because high-quality spectra were not obtained in the microbeam XANES analysis of each particle, determination of the optimal analytical conditions is a future research target.

Supplementary Information The online version contains supplementary material available at https://doi.org/10.1007/s10163-023-01632-9.

Acknowledgements The synchrotron radiation experiments were performed at BL37XU in SPring-8 (approval no. 2019B1019). This research was supported by the Environment Research and Technology Development Fund (JPMEERF20143K02, JPMEERF20173001, and JPMEERF20S20601) of the Environmental Restoration and Conservation Agency provided by the Ministry of Environment of Japan. We would like to thank Dr. Akira Sano for technical assistance with the experiment.

Data availability The datasets generated and/or analyzed during the current study are available from the corresponding author on reasonable request.

References

1. UN Environment Programme (2022) Minamata Convention on Mercury , Overview, https://www.mercuryconvention.org/en/parties/overview (2022, 12.1 accessed)
2. Takaoka M (2015) Mercury and mercury-containing waste management in Japan. J Mater Cycles Waste Manag 17:665–672
3. Sodeno R, Takaoka M (2017) Prediction of surplus mercury in the world and Japan after adoption of Minamata convention. J. Japan Soc. Civil Eng Ser G (Environmental Research) 73:112–120 **(in Japanese)**
4. US Department of Energy (2011) Long-term management and storage of elemental mercury, Environmental Impact Statement, January 2011, http://energy.gov/sites/prod/files/ EIS-0423-FEIS-Summary-2011.pdf
5. GÖSSNITZER A, (2020) Mercury management along the chain from remediation to final storage: principles facilitating the development of beneficial mercury thresholds, Global Environ. Res 24:59–64
6. Fuhrmann M, Melamed D, Kalb PD, Adams JW, Milian LW (2002) Sulfur polymer solidification/stabilization of elemental mercury waste. Waste Manag 22:327–333
7. Hagemann S (2009) Technologies for the stabilization of elemental mercury and mercury-containing wastes, Gesellschaft für Anlagen-und Reaktorsicherheit (GRS) Final Report 252
8. Fukuda N, Takaoka M, Oshita K, Mizuno T (2014) Stabilizing conditions of metal mercury in mercury sulfurization using a planetary ball mill. J Hazard Mater 276:433–441
9. Kusakabe T, Takaoka M (2020) Sulfurization and solidification of wastes consisting of elemental mercury. Global Environ. Res. 24:27–33
10. Anna M, Andrey F, Eugenia V (2022) Comparison of the performance of different methods to stabilize mercury-containing waste. J Mater Cycles Waste Manag 24:1134–1139
11. Yanase R, Hirata O, Matsufuji Y, Hanashima M (2009) Behavior of mercury from used batteries in landfills over 20 years. Haikibutsu Gakkaishi 20:12–23 (**(in Japanese)**)
12. Sano A, Kawase K, Yanase R, Takaoka M, Matsuyama A, Takahashi F, Kato T (2020) Long-term mercury behavior in sulfurized/Solidified mercury wastes by a simulated landfill experiment using lysimeters, Global Environ. Res 24:35–43
13. Hirata O, Yanase R, Kawase K, Takaoka M, Kusakabe T, Takahashi F (2021) Long-term mercury behavior in mercury waste by a simulated landfill lysimeter -Mass balance of mercury dissolution and diffusion with different landfilled patterns and waste types, Proc. 18th Inter. Symposium on Solid Waste Manag. and Sustainable Landfilling (Sardinia 2021)
14. Lindberg SE, Wallschläger D, Prestbo EM, Bloom NS, Price J, Reinhart D (2001) Methylated mercury species in municipal waste landfill gas sampled in Florida, USA. Atmos Environ 35:4011–4015
15. Gworek B, Dmuchowski W, Gozdowski D, Koda E, Osiecka R, Borzyszkowski J (2015) Influence of a municipal waste landfill on the spatial distribution of mercury in the Environment. PLoS ONE 10:e0133130
16. Lee SW, Lowry GV, Kim HH (2016) Biogeochemical transformations of mercury in solid waste landfills and pathways for release. Envrion Sci Processe Impacts 18:176–189

17. Tao Z, Deng H, Li M, Chai X (2020) Mercury transport and fate in municipal solid waste landfills and its implications. Biogeochemistry 148:19–29
18. Earle CDA, Rhue RD, Earle JFK (1999) Mercury in a municipal solid waste landfill. Waste Manag Res 17:305–312
19. Yang J, Takaoka M, Sano A, Matsuyama A, Yanase R (2018) Vertical distribution of total mercury and mercury methylation in a landfill site in Japan. Inter J Environ Res Public Health 15:1252
20. Xiong Y, Takaoka M, Kusakabe T, Shiota K, Oshita K, Fujimori T (2020) Mass balance of heavy metals in a non-operational incinerator residue landfill site in Japan. J Mater Cycles Waste Manag 22:354–364
21. Sato M, Ishigaki T, Endo K, Yamada M (2020) Emission control of mercury from stabilized and solidified products under monofill conditions, Global Environ. Res 24:3–10
22. Ishimori H, Hasegawa R, Ishigaki T (2021) Long-term leaching and volatilization behavior of stabilized and solidified mercury metal waste. J Mater Cycles Waste Manag 23:741–754
23. Terzano R, Santoro A, Spagnuolo M, Vekemans B, Medici L, Janssens K, Göttlicher J, Denecke MA, Mangold S, Ruggiero P (2010) Solving mercury (Hg) speciation in soil samples by synchrotron X-ray microspectroscopic techniques. Environ Pollut 158:2702–2709
24. Liem-Nguyen V, Skyllberg U, Bjorn E (2017) Thermodynamic modeling of the solubility and chemical speciation of mercury and methylmercury driven by organic thiols and micromolar sulfide concentrations in boreal wetland soils Environ. Sci Technol 51:3678–3686
25. Kim CS, Rytuba JJ, Brown GE (2004) Geological and anthropogenic factors influencing mercury speciation in mine wastes: an EXAFS spectroscopy study. Appl Geochem 19:379–393
26. Bernaus A, Gaona X, Esbrí JM, Higueras P, Falkenberg G, Valiente M (2006) Microprobe techniques for speciation analysis and geochemical characterization of mine environments: the mercury district of Almadén in Spain. Environ Sci Technol 40:4090–4095
27. Ohashi H, Yamazaki H, Yumoto H, Koyama T, Senba Y, Takeuchi T, Terada Y, Suzuki M, Kawamura N, Mizumaki M, Nariyama N, Takeshita K, Fujiwara A, Uruga T, Goto S, Yamamoto M, Takata M, Ishikawa T (2013) Stable delivery of nano-beams for advanced nano-scale analyses. J Phys Conf Ser 425:052018
28. Ravel B, Newville M (2005) ATHENA, ARTEMIS, HEPHAESTUS: data analysis for X-ray absorption spectroscopy using IFEFFIT. J Synchrotron Radiat 12:537–541. https://doi.org/10.1107/S0909049505012719
29. Takaoka M, Shiono A, Nishimura K, Yamamoto T, Uruga T, Takeda N, Tanaka T, Oshita K, Matsumoto T, Harada H (2005) Dynamic change of copper in fly ash during de novo synthesis of dioxins. Environ Sci Technol 39:5878–5884
30. Takaoka M, Takeda N, Yamamoto H, Nagoshi M, Fujisawa Y (2002) Chemical bonding of mercury in municipal solid waste incinerator fly ash, Proc. of the 13th Annual Conf of the Japan Soc of Waste Manag. Experts: 881–883 (in Japanese)
31. Vogel C, Krüger O, Herzel H, Amidani L, Adam C (2016) Chemical state of mercury and selenium in sewage sludge ash based P-fertilizers. J Hazard Mater 313:179–184
32. Kusuyama E, Hidari K, Kamura K (2020) Effectiveness of resistivity monitoring for unsaturated water flow in landfill sites. J Mater Cycles Waste Manag 22:2029–2038
33. Isobe Y, Ishimori H, Ishigaki T, Yamada M (2022) A study on the exploring water pathway in landfill using the electrical resistivity survey monitoring, Proc of the 33rd Annual Conf of Japan Society of Mater. Cycles and Waste Manag. https://doi.org/10.3985/jjsmcwm.33.39
34. Terashima Y, Naito S (1989) Behavior and prediction of water and pollutants in a solid waste bed–As a basis for predicting the leachate quantity and quality in a landfill site, Proc. of Environ. & Sani. Eng Res 25:1–13 **(in Japanese)**
35. Drott A, Björn E, Bouchet S, Skyllberg U (2013) Refining thermodynamic constants for mercury(II)-sulfides in equilibrium with metacinnabar at sub-micromolar aqueous sulfide concentrations. Environ Sci Technol 47:4197–4203
36. Dickson FW, Tunell G (1959) The stability relations of cinnabar and metacinnabar. Am Miner 44:471–487